Educational and Applied Contributions in Energy System Optimization Using a YALMIP-Based MILP Framework

Matej Ivaniček[1], Josipa Tisaj[2] and Markus Lehner[3]

[1]Zagreb School of Economics and Management, Croatia, matej.ivanicek@zsem.hr
[2] Chair of Process Technology and Industrial Environmental Protection, Montanuniversität Leoben, Austria, josipa.tisaj@stud.unileoben.ac.at
[3]Chair of Process Technology and Industrial Environmental Protection, Montanuniversität Leoben, Austria, markus.lehner@stud.unileoben.ac.at

*These authors contributed equally to this work.

Abstract

As the energy sector undergoes rapid decarbonization, the design and operation of Integrated Energy Systems (IES) that combine various energy vectors including electricity, natural gas, hydrogen, heating, and cooling systems are becoming essential components of modern infrastructure. Within such systems, Power-to-Gas (PtG) acts as a key coupling technology that enables flexible sector integration by converting surplus renewable electricity into hydrogen or synthetic methane. Modelling and optimizing such systems often require advanced mathematical formulations that, while rigorous, can be challenging for students to grasp, particularly when expressed in traditional matrix notation. This paper proposes the use of Yet Another Linear Matrix Inequality Parser (YALMIP)-based teaching framework, a Matrix Laboratory (MATLAB)-based optimization modelling toolbox, as an intuitive and pedagogically effective platform for introducing optimization in IES. Compared to traditional approaches that require matrix-based formulation (e.g., specifying cost vectors and constraint matrices), YALMIP allows students to directly express constraints and objectives in natural, equation-based form, which aligns closely with how such problems are conceptually taught and understood. Using a dynamic mixed-integer linear programming (MILP) model of an IES that incorporates PtG as a coupling component and that includes renewable energy prioritization, grid emission factors, and CO_2 cost penalties, reflecting current energy transition policies and constraints, this paper presents a custom-formulated optimization framework for an IES, and it illustrates how students can explore real-world operational trade-offs. While this material has not yet been implemented in classroom instruction, it is presented as a proof of concept for teaching with the potential to support future course integration or serve as a basis for applied student assignments.

Keywords: *IES, PtG, Optimization, YALMIP, MILP, Energy System Modeling, Teaching, Education.*

ISSN 2991-9371

1. Introduction

Learning how to formulate and solve optimization problems has long been recognized as a major challenge for students. Kintsch [1] provides a detailed overview of text comprehension theories in the context of solving arithmetic and algebra word problems, stating that students encounter the greatest difficulty when formulating a mathematical model of the problem, and determining whether the formulated model is correct. Kintsch [1] also emphasizes the importance of supporting the formulation stage, as students often jump to equations without a clear understanding of the problem structure. Moreover, while experienced problem solvers habitually check the reasonableness of their results, novice learners often fail to do so, producing implausible values without recognizing that their solution is incorrect. Comparable difficulties are highlighted by Stevens and Palocsay [2], who report that students, particularly those without a strong mathematical background, frequently rush into writing algebraic expressions by imitating textbook examples, without a deeper understanding of what the variables represent or how the constraints reflect the problem's structure. Similar obstacles can arise in the use of Matrix Laboratory (MATLAB) for optimization because problems must be reformulated into strict mathematical notation before solvers can be invoked. While mathematically rigorous, this approach introduces an additional layer of abstraction that may hinder conceptual understanding. This observation is supported in the work of Astutik and Fitriatien [3] that found that students learning linear programming (LP) with MATLAB struggled significantly due to the requirement of rewriting problems into canonical form. *Yet Another Linear Matrix Inequality Parser* (YALMIP) provides an alternative that lowers these barriers. It enables users to declare decision variables, constraints, and objectives directly in MATLAB using commands that closely mirror natural mathematical expressions, thereby removing the need for manual transformations. This allows learners to focus on the principles of optimization rather than on the technicalities of algebraic reformulation. The effectiveness of this approach has been demonstrated in control education with Pakshin and Emelianova [4] reporting that students using YALMIP and Self-Dual-Minimization (SeDuMi) to address real-world problems such as aircraft stabilization achieved faster progress and a deeper understanding of modern control techniques, precisely because the modelling environment emphasized conceptual reasoning rather than syntax. In line with this, this work also aims to highlight the pedagogical value of YALMIP, but through the formulation and solution of a Mixed-Integer Linear Programming (MILP) problem in the context of an Integrated Energy System (IES) with Power-to-Gas (PtG). MILP represents the most straightforward and widely studied form of optimization, and it is therefore the natural first step when learning how to model and solve optimization problems. The choice of IES with PtG as the case study is not arbitrary. Energy systems provide a rich, real-world context in which optimization plays a decisive role, while at the same time they are at the centre of global efforts to decarbonize. The urgency of decarbonizing energy systems arises from the global climate crisis and the ongoing energy transition. In 2019, fossil fuels still dominated global final energy consumption, accounting for over two-thirds of the mix (IEA [5]). Their use remains tightly linked to greenhouse gas emissions, which totaled about 59 ± 6.6 gigatonnes of carbon dioxide equivalent (Gt CO_2-eq) in the same year, with CO_2 from fossil combustion and industry as the largest contributor (IPCC [6]). The Paris Agreement calls for deep transformation to limit warming to below 2 °C, ideally 1.5 °C. Renewable electrification is central to this transition, but many sectors still require energy-dense fuels. PtG offers a pathway by converting renewable electricity into

ISSN 2991-9371

hydrogen or synthetic natural gas (SNG), which can be stored and transported in existing gas grids. Wu et al. [7] describe PtG as a coupling element within IES, connecting electricity, gas, hydrogen, and heat networks. A key pathway is CO_2 methanation [8–10], where renewable hydrogen reacts with CO_2 to produce SNG. Reiter and Lindorfer [11] emphasize that sustainability depends on the CO_2 source, and biogenic origins such as biogas upgrading make the process nearly carbon-neutral. Because IES integrates electrolyzers, renewable inputs, CO_2 capture, methanation, and storage, they require advanced control and optimization. Liang et al. [12] applied particle swarm optimization to coordinate electricity and gas networks, while Yang et al. [13] proposed an integrated Carbon Capture Storage (CCS), PtG and Combined Heat and Power (CHP) framework using YALMIP and Interior Point Optimizer (IPOPT). Liang et al. [14] later introduced reinforcement learning (TD3) for adaptive management. Shao et al. [15] developed a MILP model under wind uncertainty, Wang et al. [16] combined process and system optimization for methanation, Calsie et al. [17] analyzed system sizing, and Sun et al. [18] and Zheng et al. [19] incorporated electrolyzer dynamics into MILP formulations. This body of work shows that the research frontier has largely focused on developing increasingly sophisticated optimization models for optimizing different energy systems. By contrast, relatively little attention has been given to the educational dimension: how optimization can be introduced to students in a way that balances mathematical rigor with accessibility, and how tools like YALMIP can serve as a bridge between theory and application. Therefore, the purpose of this work is not to propose a new optimization algorithm, but to show how an established method such as MILP can be applied and taught more effectively through the intuitive modelling environment provided by YALMIP, thus addressing a gap at the intersection of energy systems optimization and education.

2. Practical Setup for Optimization Modeling with YALMIP

YALMIP is a free modeling toolbox for MATLAB, designed to simplify the process of defining and solving optimization problems. This chapter provides a detailed, step-by-step guide for setting up YALMIP in MATLAB, and some description of basics in YALMIP.

2.1 Installation and Setup of YALMIP

The first step is to obtain YALMIP from its official website, located at https://yalmip.github.io/download/, where the latest version is available as a compressed *.zip* archive. Once downloaded, the archive must be extracted to a known location on the user's system. After extraction, it is necessary to make MATLAB aware of the toolbox by adding it to the search path. This can be done by opening MATLAB and using the graphical interface to navigate to the extracted YALMIP folder, right-clicking it, and selecting the option *Add to Path* followed by *Selected Folders and Subfolders*. Once YALMIP has been added to the MATLAB path, it is crucial to install and configure the optimization solvers that YALMIP relies on. YALMIP itself does not solve optimization problems. It functions as a high-level modeling layer that reformulates the user's mathematical model into a form suitable for solvers. This makes it a parser rather than a solver in the classical sense. YALMIP supports a wide range of solvers, both open-source and commercial. MATLAB's *Optimization Toolbox*, if available, can be used to access basic solvers such as *linprog* and *intlinprog*. This toolbox can be installed via the *Add-Ons* menu in MATLAB.

2.2 Basics of YALMIP

The basic structure of a YALMIP model is built around symbolic definitions of variables, constraints, and an objective function, which are then passed to an external solver. The modeling process typically begins with ***yalmip ('clear')*** to remove any residual data from previous runs. Decision variables represent unknown quantities that the optimization algorithm will choose to achieve the best possible outcome, subject to the given constraints. They are declared using ***sdpvar*** for continuous variables and ***binvar*** for binary ones. These variables are symbolic and only receive numerical values after optimization. Constraints are introduced next and collected in an array. Typical constraint list begins as an empty array using ***constraints*** = [] and is then expanded using MATLAB's standard relational operators (<=,>=,==). Constraints express the rules or limits that the decision variables must obey, such as physical laws or capacity limits. These can involve symbolic matrix operations and indexing, making it easy to express time-dependent or structured systems. The objective function defines what we are trying to optimize, usually a cost that should be minimized or a profit that should be maximized. For example, minimizing energy cost or maximizing revenue from gas sales. To run the optimization, a solver is selected using ***sdpsettings***, such as ***options*** = ***sdpsettings*** ('***solver***','***bnb***'), and the problem is solved with the optimize function: ***results*** = ***optimize*** (***constraints***, ***objective***, ***options***). Since the optimize function minimizes the objective by default, maximizing requires multiplying the objective by –1 before solving. After a successful solve, numerical results are retrieved using the ***value*** function.

3. Example System for Applying YALMIP-Based MILP Optimization

After outlining the general structure of YALMIP and its modelling capabilities, this chapter presents a formulation of an IES both in *canonical form* and in YALMIP's *equation-based style*. The IES considered in this study consists of an electrolyzer, hydrogen storage, a methanation reactor, a biogas supply unit, and an electricity generation unit. The electrolyzer converts electricity, sourced from renewables or the grid, into hydrogen, operating within defined power limits. The produced hydrogen is stored in a pressurized tank with minimum and maximum capacity constraints, and it serves as a flexible energy carrier within the system. Hydrogen from storage is then used in the methanation unit, where it reacts with biogas to produce SNG and heat. The biogas unit provides the feedstock for this process and supplies biogas to a generator that produces electricity for sale to the grid. The optimisation aims to maximise profit while satisfying all technical and physical constraints.

ISSN 2991-9371

While the canonical representation is shown for comparison, the implementation and optimization are carried out exclusively in YALMIP. Table 1 provides a parallel comparison between equation-based style where constraints and objective are written directly in their algebraic form, while the right column shows their canonical matrix representation as rows of A, b, A_{eq}, b_{eq} and bounds l,u.

	Equation-based (YALMIP style)	**Canonical (matrix form)**
DV	$P_{elz}, P_{heat}, P_{cool}, P_k, P_{ren}, s, z, T, H, \alpha$ $\gg P_{elz} = sdpvar(N,1), \ldots s = binvar(N,1) \ldots$	$P\_elz \rightarrow indices\ 1 \ldots N$ $P\_heat \rightarrow indices\ N+1 \ldots 2N$ $P\_cool \rightarrow indices\ 2N+1 \ldots 3N$ $P_k \rightarrow indices\ 3N+1 \ldots 4N$
EL	$0.25 \cdot p_{rated} \cdot s(t) \leq P_{elz}(t) \leq p_{rated} \cdot s(t)$ (1) $\gg constraints\ =\ [0.25 * p_{rated} * s\ \leq\ P_{elz} \leq\ p_{rated} * s];$	$\boldsymbol{Ax \leq b}: P_{elz}(t) - p_{rated} \cdot s(t) \leq 0, 0.25 \cdot p_{rated} \cdot s(t) - P_{elz}(t) \leq 0, t = 1,2, \ldots, N$ $\gg A = [eye(N), zeros(N, 4*N), -p_{rated} * eye(N), zeros(N, 3*N)]; b = zeros(N,1)$
CH	$0 \leq P_{cool}(t) \leq m \cdot z(t)$ (2) $0 \leq P_{heat}(t) \leq m \cdot (1 - z(t))$ (3) $\gg constraints\ =\ [constraints, 0 \leq P_{cool} \leq m \cdot z];$ $\gg constraints\ =\ [constraints, 0 \leq P_{heat} \leq m \cdot (1 - z)];$	$\boldsymbol{Ax \leq b}: P_{cool}(t) - m \cdot z(t) \leq 0, P_{heat}(t) + m \cdot z(t) \leq m, t = 1,2, \ldots, N$ $\gg A = [A;\ zeros(N, 2*N), eye(N), zeros(N, 3*N), -m * eye(N), zeros(N, 3*N))]; b = [b; zeros(N,1)]$ $\gg A = [A;\ zeros(N), eye(N), zeros(N, 4*N), m * eye(N), zeros(N, 3*N)]; b = [b; m * ones(N,1)]$
PB	$P_{cool}(t) + P_{heat}(t) + n_c \cdot P_{elz}(t) = P_k(t) + P_{ren}(t)$ (4) $\gg constraints\ =\ [constraints, P_{cool} + P_{heat} + n_c \cdot P_{elz} = P_k + P_{ren}];$	$\boldsymbol{A_{eq}x = b_{eq}}$: $P_{cool}(t) + P_{heat}(t) + n_c \cdot P_{elz}(t) - P_k(t) - P_{ren}(t) = 0, t = 1,2, \ldots, N$ $\gg A_{eq} = [\,n_c * eye(N), eye(N), eye(N), -eye(N), -eye(N), ze$ $* N)]; b_{eq} = zeros(N,1)$
HD	$H(t+1) = H(t) + H_{in}(t) - H_{out}(t)$ (5) $H_{in}(t) = \frac{0.002016 \cdot n_c}{0.08988 \cdot 2 \cdot F \cdot b} \cdot \Delta t \cdot \left(P_{elz}(t) - (a \cdot T(t) + c)\right)$ (6) $H_{out}(t) = \alpha(t) \cdot 4 \cdot B \cdot CO_2 \cdot 1.02 + \alpha(t) \cdot 3 \cdot B \cdot CO \cdot 1.02 + \alpha(t) \cdot 2 \cdot B \cdot O_2 \cdot 1.02 - \alpha(t) \cdot B \cdot H_2$ (7) $\gg\ constraints\ =\ [constraints, H(t+1) = H(t) + H_{in}(t) - H_{out}(t)];$	$\boldsymbol{A_{eq}x = b_{eq}}: H(t+1) - H(t) - kPelz(t) + kaT(t) + f\alpha(t) = -kc,\ t = 1,2, \ldots, N-1$ $k = \frac{0.002016 \cdot n_c}{0.08988 \cdot 2 \cdot F \cdot b} \cdot \Delta t$ $f = 4 \cdot B \cdot CO_2 \cdot 1.02 + 3 \cdot B \cdot CO \cdot 1.02 + 2 \cdot B \cdot O_2 \cdot 1.02 -\ B \cdot H_2$ $\gg D = -eye(N) + diag(ones(N-1), 1); D\ = D(1{:}N-1, :);$ $\gg A_{eq} = \left[A_{eq};\ -k * eye(N-1, N), zeros(N-1, 3*N), -eye(N-1, N), zeros(N-1, 3*N), D, f * eye(N)\right]; b_{eq} = [b_{eq};\ -kc * ones(N,1)]$
TB	$t_{min} \cdot s(t) \leq T(t) \leq t_{max}$ (8) $\gg\ constraints\ =\ [constraints, t_{min} \cdot s \leq T \leq t_{max}];$	$\boldsymbol{Ax \leq b}: t_{min} \cdot s(t) - T(t) \leq 0, T(t) \leq t_{max}, t = 1,2, \ldots, N$ $\gg A = [A; zeros(N, 5*N), t_{min} * eye(N), zeros(N), -eye(N), zeros(N, 2*N)]; b = [b; zeros(N,1)]$

Table 1 Parallel formulation of the IES MILP problem in equation-based (YALMIP) and canonical (matrix) form.

ISSN 2991-9371

Row *decision vector* (DV) in Table 3. lists all decision variables ($P_{elz}, P_{heat}, P_{cool}, P_k, P_{ren}, s, z, T, H, \alpha$) denoting power supplied to the electrolyzer, heater and cooler, the electricity purchased from the grid or renewable sources, state of the electrolyzer and cooling system (on/off), electrolyzer temperature, hydrogen storage level and fraction of biogas routed to methanation, respectively. They are repeated over the $N= 50$ discrete time steps, with each representing one hour ($\Delta t=$ 3600 s). In YALMIP, each variable is declared as a vector of length N, while in *canonical form* all variables are stacked into a single decision vector $x \in R^{10N}$. The *electrolyzer* (*EL*) row introduces constraint for alkaline water electrolyzer (AWE) to operate between 25% and 100% of its rated power (Sun et al. [18]). This constraint (Eq. 1) is easily expressed as an inequality in YALMIP, while in canonical form it requires each inequality to be expressed in terms of coefficients for every decision variable placed in the correct positions of the block structure, and the right-hand side values collected in b. Similarly, the heating and cooling exclusivity (Eq. 2-3) introduced in *cooling/heating* (*CH*) row is easy to state in YALMIP by linking bounds to the binary variable z(t), whereas in canonical form it requires filling out matrix *A* and *b* with appropriate coefficients. m is a large constant used to define the upper limit of the possible power values. The power balance (Eq. 4) where n_c denotes the number of electrolyzer cells, appears in YALMIP as a single equality, but in canonical form it corresponds to one row of the equality matrix A_{eq}, constructed from identity blocks with positive and negative signs. Idea behind power balance equation is that at each time step, the energy consumed by the electrolyzer, the heating system, and the cooling system must equal the electricity supplied by both the grid and the renewable source. Dynamic constraints, such as hydrogen storage evolution (Eq. 5) and electrolyzer thermal dynamics (Eq. 9) illustrated in Table 1 as *hydrogen dynamics* (*HD*) and *temperature dynamics* (*TD*), also highlight the difference. In YALMIP, they can be written naturally as equalities across time steps, often inside a loop. In canonical form, these produce block matrices in A_{eqthat} couple variables across time, for example using shifted identity matrices $I_{(N-1,N)}$ or the difference operator D, with additional parameters such as k,f,e acting as multipliers. The thermal model of the electrolyzer is adopted from Sun et al. [18], with temperature T(t+1) updated by a discrete-time heat balance that accounts for internal heat generation, heating, cooling, and thermal losses, linearized following Zheng et al. [19] to fit into the MILP framework. Similarly, hydrogen storage dynamics are captured by balance equations linking input (Eq. 6) from electrolysis and output (Eq. 7) to methanation, constrained within design limits. The hydrogen input from electrolysis is derived from Faraday's law, using some scaling factors and linear approximation following Zheng et al. [19], while the hydrogen demand for methanation depends on the biogas composition and reaction stoichiometry. The coefficients 4, 3, and 2 in Eq, 7 correspond to the stoichiometric molar ratios of hydrogen required, based on fundamental reaction equations as reported by Rönsch et al. [8]. A 2% excess factor is included to ensure complete conversion. Additionally, if any hydrogen is already present in the biogas, it is subtracted from the required amount. Simple conditions like *temperature bounds* (*TB*), and other bounds illustratd in row *other bounds* (*OB*), translate in YALMIP into compact inequalities, while in canonical form they are represented through the lower and upper bound vectors l and u, filled systematically for all time steps using the replication vector $v \in R^N$. Electricity drawn from the grid is limited by a technical upper bound (Eq. 10), while the use of renewable energy is limited by its time-dependent availability e_{ren} (Eq. 11). Since α represents a proportion, it is bounded between 0 and 1 (Eq. 12). This formulation allows the optimization model to continuously shift all biogas use between methanation (α = 1) and electricity generation (α = 0), or adopt intermediate values, depending on operational costs and market prices. Hydrogen

ISSN 2991-9371

storage is also limited by upper and lower storage level (Eq. 13). Constraint (Eq. 14) as described in *renewable share* (*RS*) ensures that renewable energy maintains a minimum share γ in the total electricity consumption over the optimization horizon. Initial conditions are set for temperature t_1 and hydrogen level h_1 at the start of the simulation. Optimization focuses on maximizing the total economic benefit during operation of described IES as shown in Eq. 15 where the parameters k_{SNG} and k_m represent the economic revenue per unit of SNG and electricity generated from biogas, respectively. The cost of purchasing electricity from the grid is modelled through the term $P_k(t) \cdot p_{el}(t)$, where p_{el} is the electricity price. There is a possibility of purchasing some renewable electricity at fixed price p_{ren}. Finally, a CO_2^{pen} penalty term is included, capturing the environmental cost of carbon-intensive grid electricity.

$$\max\left(\sum_{t=1}^{N}\left(\alpha(t)\cdot B\cdot k_{SNG}+\left(1-\alpha(t)\right)\cdot B\cdot k_m-P_k(t)\cdot p_{el}(t)-P_{ren}(t)\cdot p_{ren}-P_k(t)\cdot CO_2^{pen}\right)\right) \tag{15}$$

In YALMIP, objective function can be directly written as a compact algebraic expression, while in canonical form it corresponds to the cost vector c (Eq. 16) where each coefficient is assigned to the appropriate decision variable in the stacked vector

$$c^T=\begin{bmatrix}0^T & 0^T & 0^T & -{p_{el}}^T & -p_{ren}v^T & 0^T & 0^T & 0^T & 0^T & B\cdot(K_{SNG}-K_m)v^T\end{bmatrix} \tag{16}$$

The final canonical formulation can be summarized through the matrices Eq. 17-20.

$$A=\begin{bmatrix} I & 0 & 0 & 0 & 0 & -p_{rated}I & 0 & 0 & 0 & 0\\ -I & 0 & 0 & 0 & 0 & 0.25p_{rated}I & 0 & 0 & 0 & 0\\ 0 & 0 & I & 0 & 0 & 0 & -mI & 0 & 0 & 0\\ 0 & I & 0 & 0 & 0 & 0 & mI & 0 & 0 & 0\\ 0 & 0 & 0 & 0 & 0 & t_{min}I & 0 & -I & 0 & 0 \end{bmatrix} \tag{17}$$

$$b^T=\begin{bmatrix}0^T & 0^T & 0^T & mv^T & t_{max}v^T\end{bmatrix} \tag{18}$$

$$:\begin{bmatrix} n_cI & I & I & -I & -I & 0 & 0 & 0 & 0 & 0\\ -kI_{N-1,N} & 0 & 0 & 0 & -I_{N-1,N} & 0 & 0 & 0 & D & fI_{N-1,N}\\ -\Delta t\kappa_P I_{N-1,N} & -\Delta t\eta I_{N-1,N} & \Delta tCOPI_{N-1,N} & 0 & 0 & 0 & 0 & D-eI_{N-1,N} & 0 & 0 \end{bmatrix} \tag{19}$$

$$b_{eq}=\left[0^T \quad -kc{v_{N-1}}^T \quad \Delta t\left(\kappa_O-\frac{T_{env}}{R}\right){v_{N-1}}^T\right] \tag{20}$$

These matrices are constructed from multiple building blocks: identity matrices I and shifted identity matrices $I_{(N-1,N)}$ difference matrices D, and scalar multipliers such as k,f,e. In particular, the inequality matrix A is assembled row by row, combining positive and negative identity blocks with appropriate scaling coefficients, while the equality matrix A_{eq} couples variables across successive time steps through shifted blocks and parameters. This explicit construction demonstrates the complexity of the canonical approach: every constraint must be carefully translated into coefficients of A, b, Aeq, beq making the process error-prone and less intuitive, especially when dynamic constraints are involved. By contrast, YALMIP allows constraints to be written directly in their algebraic form, greatly reducing abstraction and improving readability. For this reason, while the canonical representation has been shown here for comparison, the implementation and optimization of the model are carried out exclusively in YALMIP.

4. Results

The optimization problem was solved using the branch-and-bound (bnb) solver through YALMIP in MATLAB, and no infeasibilities were encountered. The solver returned optimal values for all decision variables, yielding a fully feasible and interpretable solution trajectory over the 50-hour discrete simulation horizon. Figure 1 displays the electricity prices used in the optimization. The dynamic grid electricity price is corrected for CO_2 emission penalties, which effectively shifts the entire price curve upward. As a result, the adjusted grid electricity price ranges from a minimum of 0.0187 €/kWh to a maximum of 0.1022 €/kWh. In contrast, the prices for renewable electricity (0.055 €/kWh), SNG (0.1 €/kWh), and heat (0.05 €/kWh) are fixed throughout the simulation period. Figure 2 illustrates the actual electricity procurement behaviour of the system. The grid purchase and renewable purchase are shown alongside the time- varying availability of renewable electricity that is visualized as a shaded area. In the early simulation hours, the system exploits periods of exceptionally low grid prices by purchasing electricity from the grid, even in the absence of available renewables. However, once grid price exceeds the renewable electricity price threshold, the system rapidly transitions to sourcing electricity exclusively from renewable sources. This shift is particularly visible during hours 12–16 and 33–40, where renewable purchase closely tracks the maximum available renewable energy, while grid purchase falls to zero. Figure 3 presents the power consumption profiles of the system's major electrical loads: the alkaline electrolyzer, the cooling unit, and the heater. Notably, the heating unit remains inactive throughout the entire simulation. The system consistently favours the operation of the cooler to heater, likely because the electrolyzer is often active which heats up the system. When comparing the power consumption in Figure 3 with the electricity procurement shown in Figure 2, a clear correspondence emerges.

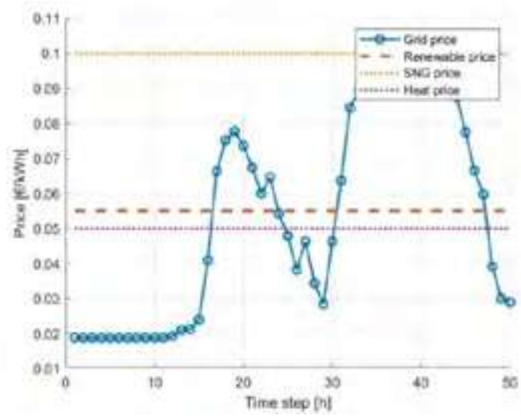

Figure 1 Time-dependent electricity and product prices used in the optimization, including grid, renewable, SNG, and heat price levels

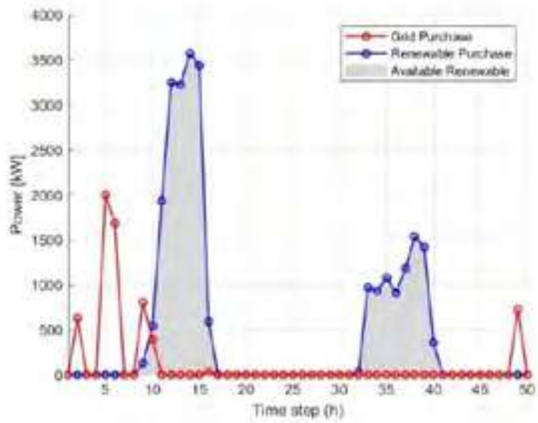

Figure 2 Comparison of purchased grid and renewable electricity with available renewable capacity over time.

The periods with high levels of renewable energy procurement, specifically hours 10–16 and 32–40, align closely with elevated power consumption by both the electrolyzer and the cooler. This correlation reflects the influence of the power balance constraint (Eq. 8), which enforces that all procured electricity must be allocated to one or more operational components. Since the heater remains inactive, the total input power is distributed between the electrolyzer and cooler. Around hour 50, there is an isolated instance of grid electricity purchase accompanied by short spikes in both electrolyzer and cooling power. Figure 4 provides an integrated view of three key operational signals: hydrogen storage level, the biogas allocation variable, and the binary on/off states of the electrolyzer and cooler. The top subplot tracks the hydrogen storage level. Initially, hydrogen level decreases steadily as α remains close to 1, indicating that all biogas is being diverted to methanation, which consumes hydrogen. This depletion continues until approximately hour 17, at which point α drops to zero and hydrogen storage begins to stabilize, suggesting that methanation halts and biogas is now routed to electricity production

ISSN 2991-9371

via the internal engine. Between hours 30 and 40, a slight rise in hydrogen storage is observed. During this period, α remains at zero, and the electrolyzer is intermittently active (as confirmed by the lower subplot), indicating hydrogen production through electrolysis while methanation remains inactive. The middle subplot reveals that α assumes values either 0 or 1, exhibiting a binary switching pattern. When grid price is high (corrected for CO_2), the optimizer favors methanation ($\alpha \approx 1$), generating revenue from SNG. Conversely, when electricity is inexpensive, the internal engine is prioritized ($\alpha \approx 0$), avoiding the costly consumption of hydrogen. The bottom subplot confirms the selective on/off operation of the electrolyzer and cooler. Finally, the system temperature evolution is shown in Figure 5.

For most of the simulation, temperature remains close to the upper limit, causing the cooler to activate intermittently. At time step 16, a sudden and sharp drop in temperature is observed. A closer look at the heat balance components at t = 15 reveals that while the electrolyzer supplied ≈ 2.08 MW of heat, the cooler extracted ≈ 2.71 MW. The net thermal balance at that moment was strongly negative (≈-0.63 MW), resulting in the pronounced temperature decline at t = 16.

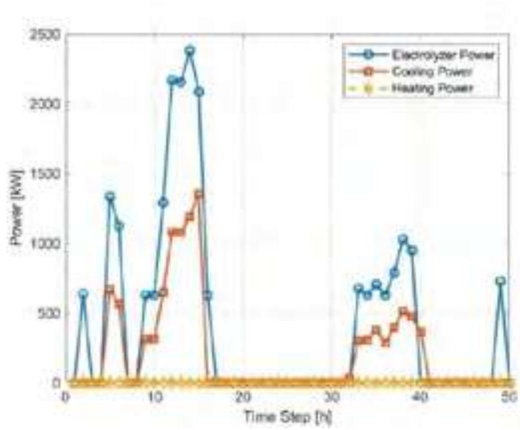

Figure 3 Power consumption of the electrolyzer, cooling, and heating systems over time.

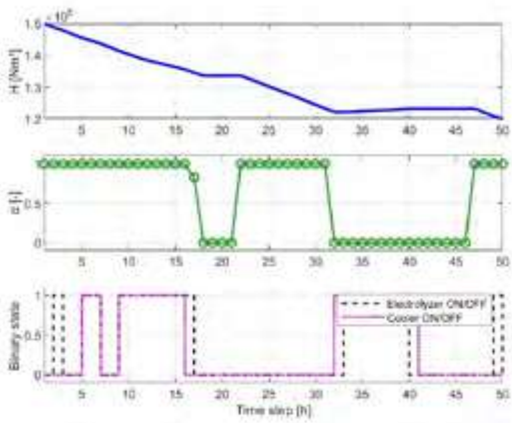

Figure 4 Time evolution of hydrogen storage level, biogas routing ratio $\alpha(t)$, and binary on/off states of the electrolyzer and cooler.

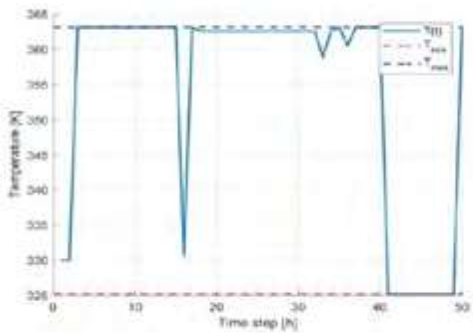

Figure 5 Electrolyzer temperature profile over time, with upper and lower operational

5. Discussion

The simulation results illustrate how the optimization model dynamically balances economic and operational constraints across electricity procurement, hydrogen storage, and thermal regulation. The system's behaviour reflects economically rational decisions, such as sourcing grid electricity when it is temporarily cheaper than renewables and switching to renewable sources once grid prices exceed a predefined threshold enforced not only by the cost structure but also by the γ-renewable constraint. The exclusive reliance on cooling, with the heater remaining unused, indicates that the system generates sufficient internal heat during electrolyzer operation to maintain acceptable temperatures. However, certain events such as the sharp temperature drop at hour 16 demonstrate that excessive cooling, especially when the system's coefficient of performance (*COP*) is high, can overcompensate and cause abrupt thermal shifts. This highlights the importance of carefully tuning cooling control logic, especially in scenarios with tight thermal constraints. The binary switching behavior of α between 0 and 1 reflects a cost-driven allocation strategy between methanation and electricity production. Internal engine for electricity generation is activated when electricity prices increase and selling electricity becomes economically attractive. These behaviours are not hardcoded into the model but emerge naturally from the optimization process as the solver continuously evaluates the marginal cost-benefit balance. A particularly illustrative moment occurs around hour 50, where a brief spike in grid electricity purchase is accompanied by corresponding increases in electrolyzer power. This isolated event likely reflects the solver exploiting a opportunity to improve the objective function, possibly due to a momentary alignment of low grid prices and favourable system conditions. Rather than representing a broader operational strategy, it highlights the optimizer's sensitivity to local variations and its ability to adapt flexibly while maintaining overall feasibility and constraint satisfaction. From a pedagogical perspective, the value of this work lies in demonstrating that advanced energy system optimization can be made accessible using intuitive modelling tools like YALMIP. By abstracting away matrix-based formulations and allowing equation-based modelling, students are free to focus on system behaviour, interdependencies, and the exploration of trade-offs. The binary decisions, energy flows, and dynamic constraints offer a rich environment for teaching real-world decision-making in energy systems. The graphical output provides intuitive feedback that reinforces learning and helps students verify model behaviour. This structure is highly adaptable to classroom and project-based learning formats, allowing students to explore extensions such as CO_2 pricing, renewable variability, and alternative objective functions.

6. Conclusion

This study developed a mixed-integer linear programming model of an integrated energy system (IES) with power-to-gas coupling and implemented it using YALMIP within MATLAB. The optimization, solved with a branch-and-bound solver over a 50-hour horizon, yielded a fully feasible and interpretable solution: dynamic electricity prices—corrected for CO_2 penalties drove the system to purchase grid power when prices were temporarily low, then switch exclusively to renewable sources once grid prices surpassed a fixed renewable threshold. The electrolyser operated in tandem with the cooling unit, while the heater remained idle, indicating that internal heat generation met thermal requirements. Hydrogen storage levels and the biogas routing variable exhibited a clear binary switching pattern; when electricity was expensive, the optimizer favoured methanation and synthetic natural gas production, whereas cheap electricity triggered the internal engine for power generation. Occasional short spikes in grid purchases illustrated the solver's responsiveness to transient price dips. Overall, the operational trajectories electricity procurement, equipment on/off states, hydrogen storage and temperature were consistent with economic and technical reasoning, demonstrating that the proposed optimization approach (OVP) works in practice and yields results that are both interesting and easily interpretable. The pedagogical contribution of this work lies in showing that YALMIP allows complex energy-system problems to be modelled using natural algebraic expressions rather than abstract matrix notation. This lowers the barrier for students, enabling them to focus on understanding system behaviour, trade-offs between cost and emissions, and dynamic constraints without being overwhelmed by formulation details. The case study highlights how YALMIP's intuitive syntax, solver integration and rich visualisation capabilities make it an effective bridge between theoretical optimisation concepts and real-world energy applications. Future work could involve empirically evaluating the framework's educational effectiveness by conducting a controlled study with students, exploring extensions to include market participation, predictive control or real-time data integration, and comparing student outcomes across different modelling tools. Such studies would provide further evidence of YALMIP's suitability as a teaching platform and inform refinements to optimise both learning and system performance.

7. References

[1] W. Kintsch, Comprehension: A Paradigm for Cognition. Cambridge, UK: Cambridge University Press, 1998, p. 364.

[2] S. P. Stevens and S. W. Palocsay, "A Translation Approach to Teaching Linear Program Formulation," INFORMS Transactions on Education, vol. 4, no. 3, pp. 38–54, May 2004. doi: 10.1287/ited.4.3.38.

[3] E. P. Astutik and S. R. Fitriatien, "Integrating MATLAB in teaching linear programming at the university level," *International Journal on Teaching and Learning Mathematics*, vol. 1, no. 2, p. 84, Dec. 2018, doi: 10.18860/ijtlm.v1i2.5882.

[4] P. Pakshin and J. Emelianova, "An Experience of Using LMI Technique in Control Education," in IFAC-PapersOnLine, Elsevier B.V., 2016, pp. 115–120. doi: 10.1016/j.ifacol.2016.07.163.

[5] International Energy Agency (IEA), Key World Energy Statistics 2021. Paris, France: IEA, 2021. [Online]. Available: https://www.iea.org/reports/key-world-energy-statistics-2021.

[6] IPCC, Summary for Policymakers, in Climate Change 2021: The Physical Science Basis. Contribution of Working Group I to the Sixth Assessment Report of the Intergovernmental Panel on Climate Change, V. Masson-Delmotte, P. Zhai, A. Pirani, S. L. Connors, C. Péan, S. Berger, et al., Eds. Cambridge, United Kingdom and New York, NY, USA: Cambridge Univ. Press, 2021, pp. 3–32. doi: 10.1017/9781009157896.001.

[7] J. Wu, J. Yan, H. Jia, N. Hatziargyriou, N. Djilali, and H. Sun, "Integrated Energy Systems," Apr. 01, 2016, *Elsevier Ltd*. doi: 10.1016/j.apenergy.2016.02.075.

[8] S. Rönsch *et al.*, "Review on methanation – From fundamentals to current projects," Feb. 15, 2016, *Elsevier Ltd*. doi: 10.1016/j.fuel.2015.10.111.

[9] A. Mazza, E. Bompard, and G. Chicco, "Applications of power to gas technologies in emerging electrical systems," Sep. 01, 2018, *Elsevier Ltd*. doi: 10.1016/j.rser.2018.04.072.

[10] C. F. Shih, T. Zhang, J. Li, and C. Bai, "Powering the Future with Liquid Sunshine," Oct. 17, 2018, *Cell Press*. doi: 10.1016/j.joule.2018.08.016.

[11] G. Reiter and J. Lindorfer, "Evaluating CO2 sources for power-to-gas applications-A case study for Austria," *Journal of CO2 Utilization*, vol. 10, pp. 40–49, Jun. 2015, doi: 10.1016/j.jcou.2015.03.003.

[12] Y. L. Liang, H. Zhang, C. T. Yang, and K. J. Li, "Research on optimization scheduling of integrated electricity-gas system considering carbon trading and P2G operation characteristics," *Electric Power Systems Research*, vol. 225, Dec. 2023, doi: 10.1016/j.epsr.2023.109797.

[13] C. Yang, X. Dong, G. Wang, D. Lv, R. Gu, and Y. Lei, "Low-carbon economic dispatch of integrated energy system with CCS-P2G-CHP," *Energy Reports*, vol. 12, pp. 42–51, Dec. 2024, doi: 10.1016/j.egyr.2024.05.055.

[14] T. Liang, L. Chai, J. Tan, Y. Jing, and L. Lv, "Dynamic optimization of an integrated energy system with carbon capture and power-to-gas interconnection: A deep reinforcement learning-based scheduling strategy," *Appl Energy*, vol. 367, Aug. 2024, doi: 10.1016/j.apenergy.2024.123390.

[15] Y. Shao, J. Wang, J. Ding, and Y. Zhang, "Stochastic scheduling optimization of integrated energy system based on hybrid power to gas and hydrogen injection into gas grid," *Int J Hydrogen Energy*, vol. 80, pp. 381–393, Aug. 2024, doi: 10.1016/j.ijhydene.2024.07.183.

[16] Y. Wang, L. Bornemann, C. Reinert, and N. von der Assen, "A method to bridge energy and process system optimization: Identifying the feasible operating space for a methanation process in power-to-gas energy systems," *Comput Chem Eng*, vol. 182, Mar. 2024, doi: 10.1016/j.compchemeng.2023.108582.

[17] F. Calise, F. L. Cappiello, L. Cimmino, M. Dentice d'Accadia, and M. Vicidomini, "Dynamic analysis and thermoeconomic optimization of a Power-to-Gas system driven by renewables," *Energy Convers Manag*, vol. 313, Aug. 2024, doi: 10.1016/j.enconman.2024.118647.

[18] J. Sun, Y. Peng, A. Wang, Q. Feng, and Y. Wang, "Optimal operation for P2H system based on a power–temperature–hydrogen coupling model for alkaline water electrolyzer plant," *Int J Hydrogen Energy*, vol. 79, pp. 150–163, Aug. 2024, doi: 10.1016/j.ijhydene.2024.06.351.

[19] Y. Zheng, S. You, H. W. Bindner, and M. Münster, "Optimal day-ahead dispatch of an alkaline electrolyser system concerning thermal–electric properties and state-transitional dynamics," *Appl Energy*, vol. 307, Feb. 2022, doi: 10.1016/j.apenergy.2021.118091.